

5-2015

Drive Plate Mass Polar Moment of Inertia in Stokeo Type Resonant Column Devices

Michael Ryan Deschenes
University of Arkansas, Fayetteville

Follow this and additional works at: <http://scholarworks.uark.edu/cveguht>

 Part of the [Civil Engineering Commons](#), and the [Structural Engineering Commons](#)

Recommended Citation

Deschenes, Michael Ryan, "Drive Plate Mass Polar Moment of Inertia in Stokeo Type Resonant Column Devices" (2015). *Civil Engineering Undergraduate Honors Theses*. 23.
<http://scholarworks.uark.edu/cveguht/23>

This Thesis is brought to you for free and open access by the Civil Engineering at ScholarWorks@UARK. It has been accepted for inclusion in Civil Engineering Undergraduate Honors Theses by an authorized administrator of ScholarWorks@UARK. For more information, please contact ccmiddle@uark.edu, drowens@uark.edu, scholar@uark.edu.

Drive Plate Mass Polar Moment of Inertia in Stokeo Type Resonant Column
Devices

An Undergraduate Honors College Thesis

in the


Department of Civil Engineering
College of Engineering
University of Arkansas
Fayetteville, AR

by

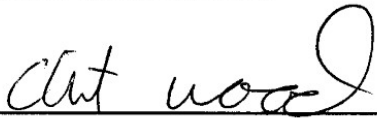
Michael Ryan Deschenes


This thesis is approved.

Thesis Advisor:



Thesis Committee:





Drive Plate Mass Polar Moment of Inertia for Stokoe-Type Resonant Column Torsional Shear Devices

Michael R. Deschenes¹, Cyrus D. Garner MSCE EIT², Inthuorn Sasanakul PhD³, Richard A. Coffman PhD PE PLS⁴

¹Undergraduate Research Assistant, Department of Civil Engineering, University of Arkansas, Fayetteville, AR 72701. mrdesche@uark.edu.

²Doctoral Candidate, Department of Civil Engineering, University of Arkansas, Fayetteville, AR 72701. cxg021@uark.edu.

³Assistant Research Professor, Department of Civil and Environmental Engineering, Rensselaer Polytechnic Institute, Troy, NY 12180. sasani@rpi.edu.

⁴Assistant Professor, Department of Civil Engineering, University of Arkansas, Fayetteville, AR 72701. rick@uark.edu.

Abstract

The calibration procedure employed by researchers at the University of Arkansas (UA) to calibrate two Stokoe-type resonant column torsional shear (RCTS) devices is presented herein. Specifically, the development of a device-specific calibration process to determine the mass polar moment of inertia of the RCTS drive plate assemblies (J_0), as a function of frequency, is described. Three aluminum calibration specimens and three stainless steel masses with known geometric and material properties were utilized to experimentally determine the J_0 values. Experimental data collected by researchers at the University of Arkansas and obtained from other sources (Utah State University, the University of Texas at Austin, the University of Colorado at Boulder, the University of Southampton, Rensselaer Polytechnic Institute, and Kleinfelder) were analyzed utilizing two different data reduction methods.

Key findings include the J_0 values for two UA drive plates ($2.743 \cdot 10^{-3} \text{ kg} \cdot \text{m}^2$ and $2.750 \cdot 10^{-3} \text{ kg} \cdot \text{m}^2$ for Devices 1 and 2, respectively) and fitted calibration functions for J_0 , as a function of frequency, for multiple RCTS devices. For samples with low natural frequencies (less than 100 Hz), the frequency dependence of the mass polar moment of inertia was determined to have negligible effects (less than 1.1 percent) on the calculated shear wave velocity for dry Ottawa sand.

Key words: Resonant Column, Calibration, Dynamic Soil Testing, Laboratory Testing

LIST OF TABLES

Table 1. Physical dimensions and material properties of calibration specimens at University of Arkansas.

Table 2. Experimentally determined mass polar moment of inertia values for the UA RCTS Device 1 (UA1) and Device 2 (UA2) drive plate assembly as obtained using the Choi (2008) and Sasanakul (2005) equations.

LIST OF FIGURES

Figure 1. Mass polar moment of inertia (J_0) as a function of frequency.

Introduction

During fixed-free resonant column torsional shear (RCTS) testing, a soil sample is fixed on one end of the sample and the free end of the sample is excited by applying a force to the sample through the RCTS drive plate assembly, resulting in deformation in first-mode torsion. The shear wave velocity (V_s), the shear modulus (G), and damping (D) of the sample may be determined, utilizing RCTS testing, after accounting for the mass polar moment of inertia of the drive plate assembly (J_0). The calibration procedure and the J_0 results, as obtained by others and as obtained using the procedures employed at the University of Arkansas (UA), are presented. Specifically, knowledge of J_0 must be developed a priori to determine the V_s and G values for a soil sample. The dynamic properties for a soil sample cannot be experimentally determined, using an RCTS device, without an accurate calculation of J_0 . The frequency dependence of the experimentally derived J_0 and the effects of the frequency dependence on the obtained value of shear wave velocity for dry Ottawa sand were evaluated and are discussed.

Background of RCTS Calibration Procedures and Results

Calibration procedures have been proposed by Sasanakul (2005), Choi (2008), Clayton et al. (2009), Sasanakul and Bay (2010), and Khosravi (2011). The aforementioned researchers utilized an experimental technique to determine the system response by coupling the drive plate to metallic calibration specimens with known values of J_0 . Specifically, Sasanakul (2005), Choi (2008), Kasantikul (2009), Sasanakul and Bay (2010), Khosravi (2011), and Laird (2013) used aluminum, brass, or steel specimens with different resonant frequencies coupled with additional stainless steel weights. Whereas, Clayton et al. (2009) utilized four aluminum calibration specimens without any additional weights.

Materials and Calibration Procedures

In 2010, the University of Arkansas (UA) acquired two Stokoe type (fixed-free) RCTS testing cells and associated instrumentation. The two devices, the data acquisition system, the operating software, and the calibration specimens were fabricated and/or assembled by Trautwein Soil Testing Equipment. Three aluminum (6061-T6) metallic calibration specimens were utilized for the calibration procedure developed at the UA. Additionally, three separate stainless steel masses (M1, M2, and M3) were utilized. The physical dimensions and properties of the calibration specimens and masses, used during the UA calibration process, are presented in Table 1.

Table 1. Physical dimensions and material properties of calibration specimens at the University of Arkansas.

Specimen	Material	Density	Diameter		Polar Mass Moment of Inertia	
		ρ g·cm ⁻³	Rod, d _r mm	Top Plate, d _t mm	Rod, J _r kg·m ²	Top Plate, J _t kg·m ²
S1	6061-T6 Al	2.700	9.53	34.93	3.900 x 10 ⁻⁷	5.036 x 10 ⁻⁶
S2	6061-T6 Al	2.700	15.88	34.93	3.009 x 10 ⁻⁶	2.253 x 10 ⁻⁶
S3	6061-T6 Al	2.700	19.05	34.93	6.240 x 10 ⁻⁶	1.846 x 10 ⁻⁶
M1	Stainless Steel 303	7.806	-	71.12 ^a	-	1.853 x 10 ⁻⁴
M2	Stainless Steel 303	7.806	-	71.12 ^a	-	1.853 x 10 ⁻⁴
M3	Stainless Steel 303	7.806	-	71.12 ^a	-	1.853 x 10 ⁻⁴

^aHeight of Mass (h_m = 9.525 mm), Masses Applied Sequentially/Simultaneously

Upon configuration of the RCTS and data collection system, test parameters were input into the National Instruments LabView (National Instruments 2013) program entitled RCSweep (Trautwein 2008). The time domain to frequency domain transformation was performed using a Fast Fourier Transform (FFT) in the RCSweep program and the approximate measured resonant frequency (f_m) was initially obtained for each specimen utilizing a large frequency span (180 Hz). Each specimen was then excited utilizing the same set of testing parameters (drive voltage of 1V, sampling rate of 1000 points, and frequency span of 10 Hz). Eight tests were performed

for each configuration. Each calibration specimen was tested sequentially, utilizing the same procedure, with zero, one, two, and three additional masses added (32 total tests per calibration specimen).

Data analyses were performed utilizing MATLAB (Mathworks 2011) on a Microsoft Windows (Microsoft 2012) platform. The respective f_m values were identified by selecting the frequency step that contained the maximum value of the transfer (amplitude) function for the corresponding specimens. Similarly, damping was determined utilizing the half power bandwidth method as described in Sasanakul (2005). Averaged resonant frequency (\bar{f}_m) and averaged damping ratio (\bar{D}) values, for a specific test configuration, were developed by determining the mean value of the calculated values of f_m and D (as calculated for each of eight redundant tests). J_0 was then calculated using Equation 1 (neglecting damping) or Equations 2 and 3 (accounting for damping). Furthermore, the value of J_0 and the value of the average resonant frequency (e.g. the average of \bar{f}_m for test i and test j in each specific comparison) were calculated for each of the 18 possible cases presented in Table 2. For each metallic calibration sample, the three values with the highest correlation were selected as valid test results (as proposed by Sasanakul 2005). Empirical calibration functions that describe the frequency dependence of J_0 , with a mathematical form similar to the function proposed by Sasanakul (2005), were also calculated for the selected calibration results.

Table 2. Experimentally determined mass polar moment of inertia values for the UA RCTS Device 1 (UA1) and Device 2 (UA2) drive plate assembly as obtained using the Choi (2008) and Sasanakul (2005) equations.

Specimen	Compared Masses		Average Resonant Frequency		Moment of Inertia ^a		Moment of Inertia ^b	
			f_m Hz		Jo kg-m ²		Jo kg-m ²	
	Series 1	Series 2	UA1	UA2	UA1	UA2	UA1	UA2
1	S1NM ^{c,d}	S1M1	32.39	32.26	2.837 x 10 ⁻³	2.871 x 10 ⁻³	2.818 x 10 ⁻³	2.933 x 10 ⁻³
	S1NM	S1M1&2	32.91	31.77	2.794 x 10 ⁻³	2.812 x 10 ⁻³	2.794 x 10 ⁻³	2.781 x 10 ⁻³
	S1NM	S1M1,2,3	31.46	31.33	2.771 x 10 ⁻³	2.790 x 10 ⁻³	2.771 x 10 ⁻³	2.787 x 10 ⁻³
	S1M1	S1M1&2	31.39*	31.25*	2.767 x 10 ⁻³	2.767 x 10 ⁻³	2.767 x 10 ⁻³	2.723 x 10 ⁻³
	S1M1	S1M1,2,3	30.94*	30.82*	2.744 x 10 ⁻³	2.753 x 10 ⁻³	2.744 x 10 ⁻³	2.760 x 10 ⁻³
	S1M1&2	S1M1,2,3	30.46*	30.33*	2.718 x 10 ⁻³	2.738 x 10 ⁻³	2.718 x 10 ⁻³	2.802 x 10 ⁻³
2	S1NM	S1M1	88.60	88.03	3.249 x 10 ⁻³	3.188 x 10 ⁻³	3.249 x 10 ⁻³	3.185 x 10 ⁻³
	S1NM	S1M1&2	87.29	86.74	3.021 x 10 ⁻³	2.999 x 10 ⁻³	3.021 x 10 ⁻³	3.001 x 10 ⁻³
	S1NM	S1M1,2,3	86.08	85.53	2.946 x 10 ⁻³	2.934 x 10 ⁻³	1.962 x 10 ⁻³	1.951 x 10 ⁻³
	S1M1	S1M1&2	86.05*	85.48*	2.797 x 10 ⁻³	2.810 x 10 ⁻³	2.797 x 10 ⁻³	2.817 x 10 ⁻³
	S1M1	S1M1,2,3	84.84*	84.28*	2.789 x 10 ⁻³	2.800 x 10 ⁻³	2.789 x 10 ⁻³	2.793 x 10 ⁻³
	S1M1&2	S1M1,2,3	83.53*	82.98*	2.780 x 10 ⁻³	2.789 x 10 ⁻³	2.780 x 10 ⁻³	2.767 x 10 ⁻³
3	S1NM	S1M1	124.97	125.08	4.428 x 10 ⁻³	3.819 x 10 ⁻³	4.428 x 10 ⁻³	3.780 x 10 ⁻³
	S1NM	S1M1&2	123.16	123.25	3.524 x 10 ⁻³	3.287 x 10 ⁻³	3.524 x 10 ⁻³	3.273 x 10 ⁻³
	S1NM	S1M1,2,3	121.47	123.25	3.280 x 10 ⁻³	3.175 x 10 ⁻³	3.524 x 10 ⁻³	3.273 x 10 ⁻³
	S1M1	S1M1&2	121.86*	121.73*	2.862 x 10 ⁻³	2.839 x 10 ⁻³	2.862 x 10 ⁻³	2.842 x 10 ⁻³
	S1M1	S1M1,2,3	120.17*	120.11*	2.839 x 10 ⁻³	2.884 x 10 ⁻³	2.839 x 10 ⁻³	2.885 x 10 ⁻³
	S1M1&2	S1M1,2,3	118.35*	118.28*	2.813 x 10 ⁻³	2.936 x 10 ⁻³	2.813 x 10 ⁻³	2.935 x 10 ⁻³

^aAs Obtained Using Choi (2008) Equation.

^cS Represents Sample Number, M Represents Mass Number.

^bAs Obtained Using Sasanakul (2005) Equation.

^dNM Represents Specimen with No Additional Mass Added.

*Indicates Test Values Utilized In Calibration Function.

$$J_0 = \frac{\Delta J_j}{\left(\frac{\bar{f}_{mi}}{\bar{f}_{mj}}\right)^2 - 1} - J_t - \Delta J_1 \frac{\left(\frac{\bar{f}_{mi}}{\bar{f}_{mj}}\right)^2}{\left(\frac{\bar{f}_{mi}}{\bar{f}_{mj}}\right)^2 - 1} \quad (\text{modified from Choi 2008}) \quad [1]$$

$$J_0 = \frac{\Delta J_j}{A-1} - J_t - \frac{A \Delta J_i}{A-1} \quad (\text{modified from Sasanakul 2005}) \quad [2]$$

$$A = \left(\left(\frac{\bar{f}_{mi}}{\sqrt{1-\bar{D}_i^2}} \right) \left(\frac{\bar{f}_{mj}}{\sqrt{1-\bar{D}_j^2}} \right)^{-1} \right)^2 \quad (\text{modified from Sasanakul 2005}) \quad [3]$$

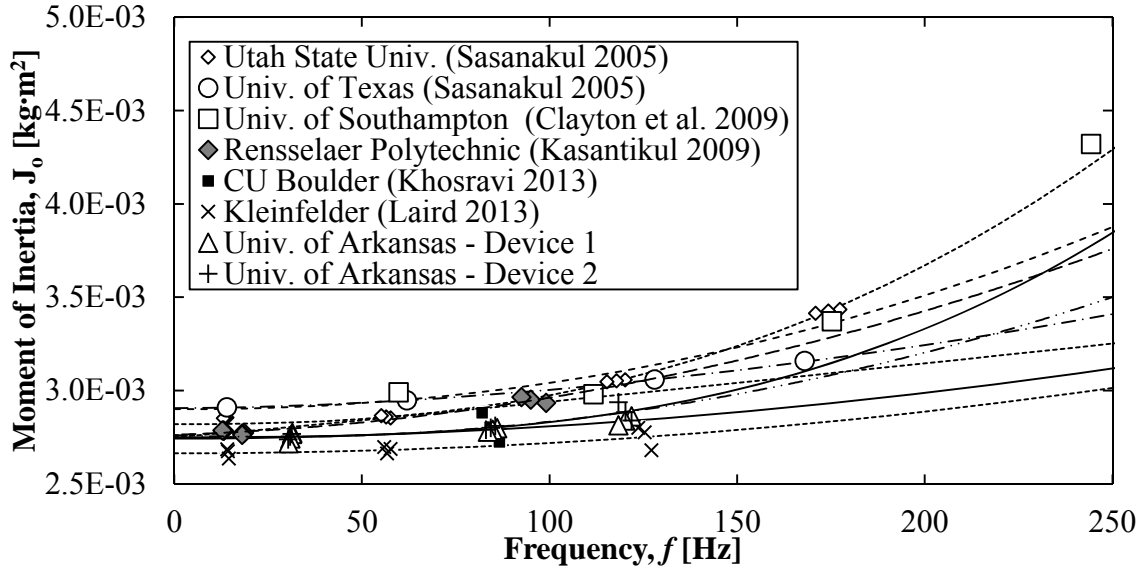
Within Equations 1 through 3, J_0 is the mass polar moment of inertia of the drive plate assembly; J_t is the calculated mass polar moment of inertia for a calibration specimen; $\bar{f}_{mi,j}$ is the average measured resonant frequency of Tests i or j ; $\Delta J_{i,j}$ is the added mass for Test i or j (ΔJ_i is null if Test i is specimen only); $\bar{D}_{i,j}$ is the averaged damping of Test i or j ; and A is an assigned quantity as defined in Equation 3.

Results

The experimentally determined \bar{f}_m for each of the 12 calibration tests performed on the UA RCTS devices (Devices UA1 and UA2) are presented in Table 2. Measured resonant frequency values of 32.9, 89.8, and 126.3 Hz were obtained for Specimens 1, 2, and 3, respectively, during the calibration of UA RCTS Device 1. During the calibration of UA RCTS Device 2, measured resonant frequencies values of 32.8, 89.3, and 126.6 Hz were obtained for calibration Specimens 1, 2, and 3, respectively. The maximum material damping coefficient for each test was less than 1.12 percent and ranged from 0.37 to 0.81 percent for UA RCTS Device 1 and 0.28 to 1.12 percent for UA RCTS Device 2.

The calculated values of J_0 for each of the 18 cases that were compared for each UA RCTS Device are also presented in Table 2 (UA RCTS Devices 1 and 2), and graphically presented in Figure 1. The maximum percent deviation between the Sasanakul (2005) and Choi (2008) methods was for UA Specimen 2 (when comparing the specimen with no mass added to the specimen with masses M1, M2, and M3 added), with a deviation value of 50.13 percent difference. However, by employing the method previously described by Sasanakul (2005), the maximum difference between the test results employed in the calibration function was 0.063 percent (with an average difference of 0.008 percent and a standard deviation of 0.016 percent). Therefore, due to the low values of device-derived material damping for the metallic calibration specimens, the effects of device-derived damping were found to be negligible. These negligible levels of device-derived damping are also anticipated to hold true for the other published and unpublished relationships (Utah State University [USU], University of Texas [UT], University of Southampton [US], Rensselaer Polytechnic Institute [RPI], and Kleinfelder calibration functions) presented by Sasanakul (2005), Clayton et al. (2009), Kasantikul (2009), and Laird (2013).

Figure 1. Mass polar moment of inertia (J_0) as a function of frequency.



The power function fitted to the frequency dependent, experimentally determined J_0 values for UA RCTS Devices 1 and 2 are presented as Equation 4 and Equation 5, respectively. The J_0 value for the UA RCTS Device 1 was numerically smaller than the J_0 values found by Sasanakul (2005), Clayton et al. (2009), and Kasantikul (2009) for the respective drive plate assemblies located at USU, UT, US, and RPI. The value of the at rest mass polar moment of inertia for the drive plates of the UA RCTS Device 2 and the RPI device are equal ($2.750 \cdot 10^{-3} \text{ kg} \cdot \text{m}^2$). The UA J_0 values and experimentally determined calibration functions were found to closely match the unpublished Kleinfelder calibration curve (Laird 2013). The close correlation between the UA and Kleinfelder calibration functions was anticipated due to the fact that the Kleinfelder apparatus and both of the UA apparatuses are of the same make and model and were therefore expected to have similar physical properties.

$$J_0 = 0.002743 + 9.7408 \cdot 10^{-9} \cdot \bar{f}_{i,j}^{1.912} \quad (\text{calibration for UA RCTS Device 1}) \quad [4]$$

$$J_0 = 0.002750 + 1.6513 \cdot 10^{-10} \cdot \bar{f}_{i,j}^{2.8447} \quad (\text{calibration for UA RCTS Device 2}) \quad [5]$$

Utilizing the fitted power function, the at rest J_0 values of $2.820 \cdot 10^{-3}$, $2.906 \cdot 10^{-3}$, $2.900 \cdot 10^{-3}$, $2.750 \cdot 10^{-3}$, $2.703 \cdot 10^{-3}$, $2.644 \cdot 10^{-3}$, $2.743 \cdot 10^{-3}$ and $2.750 \cdot 10^{-3}$, in units of $\text{kg} \cdot \text{m}^2$, were obtained for the USU, UT, US, RPI, University of Colorado, Kleinfelder and UA drive plate assemblies, respectively. Reduced frequency dependence was observed for the UA RCTS devices over frequency spans from 32 to 126 Hz. However, the determined exponential component of 1.912 is consistent with the exponential values provided for the UT (1.7843) and US (2.1124) drive plate assemblies. The fitted calibration for UA RCTS Device 2 was found to have frequency dependence that was similar to the curve presented in Sasanakul (2005). The calibration functions for the UA RCTS Device 2 device and the USU device were found to have similar frequency dependence based on the similarity between the obtained exponential values (2.4604 and 2.8447, respectively).

The variance in the individual device calibration functions was pronounced and rapidly increased at frequencies greater than 125 Hz. The frequency dependence on the J_0 value, for the drive plate assembly, has been theorized to be attributed to the type of connection used between drive plate and magnets. Specifically, at higher frequencies, the movement of the drive plate and the magnet system no longer behave as a rigid body (Sasanakul 2005). Even though this frequency dependence is a real phenomenon, the use of an exponential function may further exacerbate the effect at high frequencies (>125 Hz) because the measured resonant frequencies of the calibration specimens ranged between 10 and 125 Hz and the power functions were used to extrapolate the functions to higher frequency values. The Clayton et al. (2009) calibration procedure is the exception because it was developed for stiff samples (methane hydrates) and therefore used calibration samples with resonant frequencies exceeding 200 Hz. As a result of the divergence in calibration relationships at higher frequencies, it is recommended that the

expected range of resonant frequency values for soil samples be bounded by the values of resonant frequency for the calibration samples.

Obtained shear wave velocity values for dry Ottawa sand samples, as obtained using the measured J_0 calibration function for the UA RCTS Device 1, were found to negligibly deviate from the values obtained using the measured, at rest, J_0 value (less than 1.1 percent deviation at 95 Hz). The effects of frequency dependence were evaluated using measured shear wave velocities and the void ratio to shear wave velocity relationship proposed by Robertson et al. (1995) for void ratios of 0.1 to 1.0. It was found that correcting for the drive plate moment of inertia at the resonant frequency of the sample was not required for the range of frequencies required for soft ground testing (0-100 Hz). Although the frequency dependence is of minimal significance for low frequencies, it should be considered because it is obtained during normal calibration procedures (i.e. there is no disadvantage to considering the frequency dependence). Furthermore, for stiff samples with natural frequency values in excess of 100 Hz (e.g. those tested by Clayton et al. 2009), the effects of frequency dependence on J_0 values and therefore V_s values becomes more significant.

Conclusions

The empirical calibration of the RCTS device is a critical step for obtaining measurements of dynamic soil properties using a RCTS device. The RCTS calibration procedure employed at the University of Arkansas was presented and described. The results obtained from the UA calibration procedure were compared with data from published RCTS calibration studies conducted by Sasanakul (2005), Choi (2008), Clayton et al. (2009), Kasantikul (2009), Khosravi (2011), and Laird (2013). Specifically, the experimentally derived values of mass polar moments of inertia ($2.743 \cdot 10^{-3} \text{ kg} \cdot \text{m}^2$ and $2.750 \cdot 10^{-3} \text{ kg} \cdot \text{m}^2$) of the UA RCTS drive plates were lower than

the calibration functions presented for RCTS devices currently in use at USU ($2.820 \cdot 10^{-3} \text{ kg} \cdot \text{m}^2$), the UT ($2.906 \text{ kg} \cdot \text{m}^2$), and the US ($2.900 \cdot 10^{-3} \text{ kg} \cdot \text{m}^2$). The closest agreement between the mass polar moment of inertia for the UA RCTS devices and the values found in the literature was found to be with the RPI and Kleinfelder RCTS devices that possessed mass polar moment of inertia values of $2.750 \cdot 10^{-3} \text{ kg} \cdot \text{m}^2$ and $2.644 \cdot 10^{-3} \text{ kg} \cdot \text{m}^2$, respectively. The effects of drive plate frequency dependence on the obtained value of shear wave velocity values, for dry Ottawa sand, were found to be negligible at low frequencies but should be accounted for, because the calibrated data is available.

References

- Choi, Won Kyoung, (2008). "Dynamic Properties of Ash-Flow Tuffs." Doctoral Dissertation. University of Texas at Austin, May, 308 pgs.
- Clayton, C., Priest, J., Bui, M., Zervos, A., Kim, S., (2009). "The Stokoe Resonant Column Apparatus: Effects of Stiffness, Mass, and Specimen Fixity." *Geotechnique*, Vol. 59, No. 5, pp. 429-437.
- Kasantikul, P., (2009). "Resonant Column and Torsional Shear Testing to Evaluate Soil Properties Deposited Using Dry Pluviation and Hydraulic Fill." Masters Thesis. Rensselaer Polytechnic Institute, May, 191 pgs.
- Khosravi, Ali, (2011). "Small Strain Shear Modulus of Unsaturated, Compacted Soils During Hydraulic Hysteresis." Doctoral Dissertation. University of Colorado, May, 170 pgs.
- Laird, Joseph, (2013). "RE: Resonant Column Calibration." Personal Electronic Mail Communication with Richard A. Coffman.
- Mathworks, (2011). "MATLAB Programming Suite and Associated Documentations." Version 7.12. The Mathworks Inc. Nattick, MA.
- Microsoft, (2012). "Windows 7 Operating System and Documentation." Microsoft Corporation. Redmond, WA.
- National Instruments, (2013). "LabView Scientific Software and Supporting Documentation." National Instruments. <http://www.ni.com/labview/>. Retrieved October 2013.
- Robertson, P., Sasitharan, S., Cunning, J., Segoo, D., (1995). "Shear-Wave Velocity to Evaluate In-Situ State of Ottawa Sand." *Journal of Geotechnical Engineering*, Vol. 121, pp. 262-273.
- Sasanakul, Inthuorn, (2005). "Development of an Electromagnetic and Mechanical Model for a Resonant Column Torsional Shear Testing Device for Soils." Doctoral Dissertation. Utah State University, May, 297 pgs.
- Sasanakul, I., Bay, J., (2010). "Calibration of Equipment Damping in a Resonant Column and Torsional Shear Testing Device." *Geotechnical Testing Journal*, Vol. 33, No. 5.
- Trautwein Soil Testing Equipment Co., (2008). "Resonant Column Torsional Shear Testing Equipment and Supporting Documentation." 6909 Ashcroft Rd., Suite 104, Houston, TX 77081.